Patterns of river width and surface area revealed by the satellite-derived North American River Width data set

George H. Allen[1] and Tamlin M. Pavelsky[1]

[1]Department of Geological Sciences, University of North Carolina, Chapel Hill, North Carolina, USA

Abstract As hydraulic, hydrologic, and biogeochemical models evolve toward greater spatial resolution and larger extent, robust morphometric data sets are essential to constrain their results. Here we present the Landsat-derived North American River Width (NARWidth) data set, the first fine-resolution, continental scale river centerline and width database. NARWidth contains measurements of $>2.4 \times 10^5$ km of rivers wider than 30 m at mean annual discharge. We find that conventional digital elevation model-derived width data sets underestimate the abundance of wide rivers. To calculate the total surface area of North American rivers, we extrapolate the strong observed relationship between river width and total surface area at different river widths ($r^2 > 0.99$ for 100–2000 m widths) to narrower rivers and streams. We conservatively estimate the total surface area of North American rivers as $1.24^{+0.39}_{-0.15} \times 10^5$ km^2 (1σ confidence intervals), values 20^{+38}_{-15}% greater than previous estimates used to evaluate greenhouse gas efflux from rivers to the atmosphere.

1. Introduction

Rivers are fundamental to Earth's hydrological and biogeochemical cycles, they are biodiversity hot spots, and they provide vital water supply to human civilization. Despite their widespread importance, relatively limited empirical information on river channel form is available at continental scales to constrain river system models. These models commonly use spatially distributed measurements of river width, centerline location, and/or braiding index to estimate discharge [e.g., *Gleason and Smith*, 2014], flooding extent [e.g., *Neal et al.*, 2012], landscape evolution [e.g., *Lague*, 2014], or biogeochemical processes [e.g., *Gomez-Velez and Harvey*, 2014; *Kiel and Cardenas*, 2014; *Raymond et al.*, 2013]. As models increase in spatial resolution, extent, and sophistication, they require high-resolution, large-scale river width data sets.

A key application of these river width data sets is the estimation of the surface area of rivers at different scales. Globally, rivers are significant emitters of greenhouse gas and are estimated to outgas ~1.8 Pg C yr^{-1} of carbon dioxide [*Raymond et al.*, 2013] and ~1.5 Tg CH$_4$ yr^{-1} of methane [*Bastviken et al.*, 2011]. Among other parameters, the surface area of rivers is a primary control on gaseous efflux and is used to estimate global emission rates. Presently, the most sophisticated evaluations of global river surface area rely on (1) calculating river width from digital elevation models (DEMs) by scaling width to upstream drainage area via downstream hydraulic geometry (DHG) relationships [*Leopold and Maddock*, 1953], (2) extrapolating river width and length from large to small river basins using Horton ratios [*Horton*, 1945], and (3) extrapolating empirical relationships between climate and percentage water cover from low- to high-latitude basins where high-resolution hydrologically conditioned topographic data do not exist [*Raymond et al.*, 2013]. Because this method relies on DHG scaling, which cannot account for anthropogenic modification of riverways, it may not accurately capture the true river surface area [*Wehrli*, 2013]. Further, geographical variability in physical conditions including climate, tectonic deformation, and sediment supply and characteristics can also lead to a breakdown of DHG and climate-percentage water cover scaling [*Ferguson*, 1986; *Park*, 1977; *Wohl*, 2004].

Recent advances in image-processing algorithms have yielded large-scale, high-resolution river width surveys containing hundreds of thousands of measurements [e.g., *Allen et al.*, 2013; *Miller et al.*, 2014; *O'Loughlin et al.*, 2013; *Pavelsky et al.*, 2014a; *Yamazaki et al.*, 2014]. These compilations fall within a new class of fluvial geomorphology data sets that directly quantify river width continually downstream. Such data sets have the potential to spawn new approaches for understanding river processes in much the same way that DEMs revolutionized analysis of fluvial systems. Here we present the North American River Width (NARWidth) data set, the first continental survey of river width at mean annual discharge for rivers wider than 30 m. We analyze the

continental scale frequency distribution of river widths and compare the results to a DEM-derived width distribution. We then use the strong statistical relationship between river width and total river surface area of all rivers at that width to estimate the total surface area of North American rivers.

2. Methods

We measured river width at mean discharge from a total of 1756 Landsat scenes covering North America (see supporting information for in-depth methodology). For each Landsat path-row combination, we calculated the time of year when the observable rivers were most likely to be at mean discharge by analyzing mean monthly discharge records from the Global Runoff Data Center (GRDC) (Figure S1 in the supporting information) [*Global Runoff Data Center*, 2011]. After acquiring cloud- and river ice-free imagery from the Global Land Cover Facility (glcf.umd.edu) and the U.S. Geological Survey (USGS) (EarthExplorer. usgs.gov), we applied the modified normalized difference water index formula [*Xu*, 2006] to Landsat reflectance values and created a binary land-water mask using dynamic thresholding [*Li and Sheng*, 2012]. We visually inspected and corrected the land-water masks and calculated a channel centerline for all river reaches longer than 10 km using RivWidth software [*Pavelsky and Smith*, 2008]. RivWidth computes the river width and braiding index at each centerline pixel and outputs the data as a georeferenced vector (Figure S2 in the supporting information). We then flagged measurements of lakes and reservoirs included in the NARWidth data set using geographic information system methods and existing water body data sets (Text S1.3 in the supporting information).

Landsat-derived river width measurements were validated using 1049 geographically distributed streamflow and river width records from the U.S. Geological Survey (USGS) and the Water Survey of Canada (WSC). We included only gauges with records that (1) span at least 10 complete years of discharge measurement, (2) drain basins larger than 1000 km^2, (3) are located within 1 km of a RivWidth centerline, (4) are not immediately adjacent to reservoirs or river confluences, and (5) have river width data available. We used daily discharge measurements to calculate the in situ mean annual discharge for each location [*Kimbrough et al.*, 2003] and then compared the corresponding in situ width to the mean of the five spatially closest RivWidth measurements (Figure S3 in the supporting information).

To assess conventional width data sets built using DHG, we compared NARWidth to a DEM-derived river width data set. The DEM-derived data set was produced by *Pavelsky et al.* [2014b] to evaluate the spatial distribution of rivers observable by the planned Surface Water and Ocean Topography (SWOT) satellite mission. The data set was created using methods similar to those developed by *Andreadis et al.* [2013], except that the HYDRO1k DEM [*U.S. Geological Survey*, 2014; *Verdin and Verdin*, 1999] was used to calculate river width rather than the Hydrological data and maps based on SHuttle Elevation Derivatives at multiple Scales (HydroSHEDS) DEM [*Lehner et al.*, 2008]. This DEM-derived width data set was built by using drainage area from HYDRO1k and mean annual discharge from the GRDC in combination with a global-averaged width-discharge equation [*Moody and Troutman*, 2002] to estimate mean annual river width along HYDRO1k DEM streamlines (see *Pavelsky et al.* [2014b] for a detailed methodology description).

For both the Landsat- and DEM-derived data sets, we analyzed the distribution of river length and surface area binned by river width from 100 to 2000 m, excluding measurements of reservoirs, lakes, and Greenland rivers. River length was calculated using the Euclidean distance between each centerline pixel and the next adjacent centerline pixel. River surface area was calculated by summing the product of river width and length at each centerline pixel (Text S3 in the supporting information). We established a minimum width threshold of 100 m because we are not confident that NARWidth includes all rivers with widths below this threshold [*Miller et al.*, 2014]. We excluded rivers wider than 2000 m because they only account for 0.6% of all measurements but significantly skew the results of the analysis.

3. Results

3.1. Data Set and Validation

The North American River Width (NARWidth) data set contains 6.7×10^6 georeferenced measurements of river width ≥30 m and an additional 1.3×10^6 flagged width measurements of reservoirs and lakes that
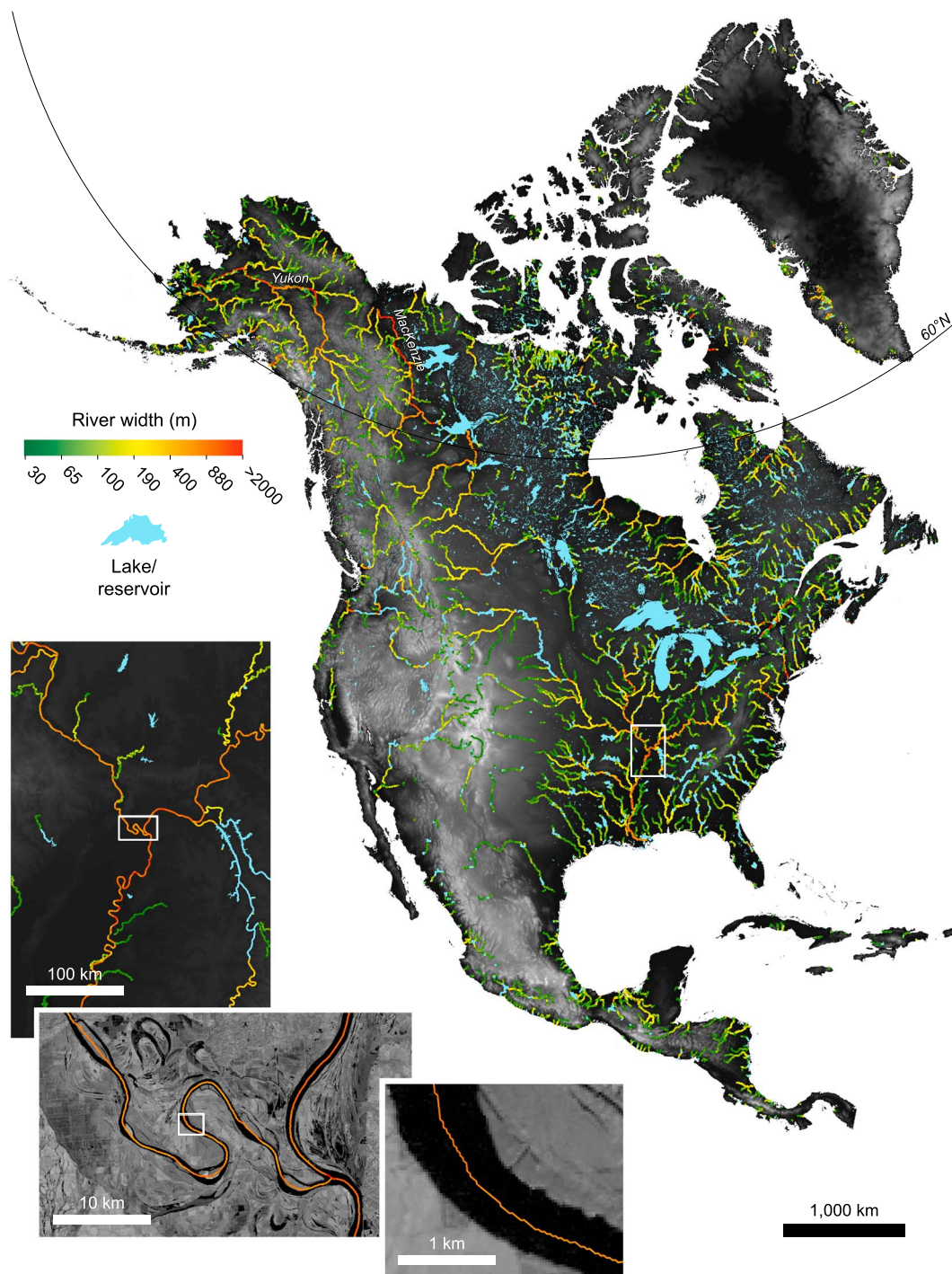
Figure 1. Map of North American river widths. The inset boxes show levels of detail available at finer spatial resolutions. Note that the color bar is stretched geometrically to accent width variability.

are connected to the fluvial network (Figure 1). In total, NARWidth measures 2.39×10^5 km of rivers with widths ≥ 30 m corresponding to a water surface area of 4.43×10^4 km^2 and 1.1×10^5 km of rivers wider than 100 m (3.64×10^4 km^2 of water surface area). NARWidth includes rivers ranging from approximately fourth to tenth Strahler stream orders [*Downing et al.*, 2012; *Strahler*, 1957]. The data set includes measurements of rivers above 60°N, where high-quality river centerline and width data are largely unavailable but excludes very large lakes (e.g., the Great Lakes), ephemeral streams, deltaic systems,
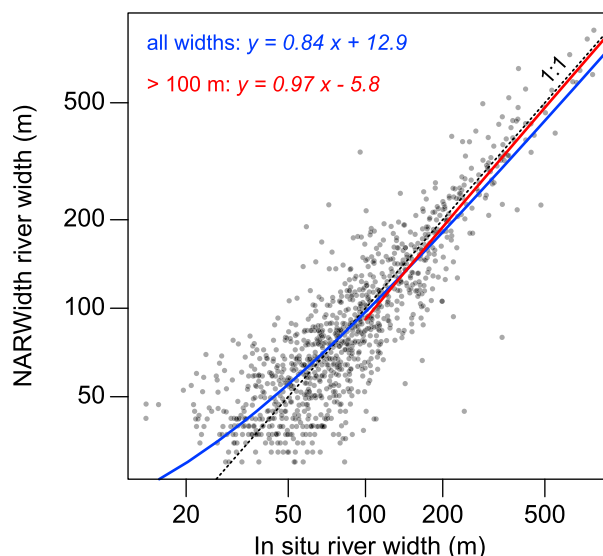
Figure 2. NARWidth validation. NARWidths were compared to USGS and WSC in situ river width measurements at 1049 locations.

and human-made canals. Additionally, NARWidth includes a braiding index field, defined as the number of channels at each river cross section. The braiding index only includes river channels wider than 30 m, a limitation imposed by the spatial resolution of Landsat imagery. NARWidth is the first continental scale morphometric survey of rivers at mean discharge and is available for download (see Acknowledgements).

NARWidth width measurements show very little mean bias (-0.35 m) relative to in situ width measurements at mean discharge, suggesting that the Landsat scenes were sampled at times that, on average, matched mean discharge timing. The root-mean-square error (RMSE) between NARWidth and in situ widths is 38.0 m, a length similar to the minimum theoretical uncertainty of Landsat-derived river widths calculated from a binary water mask [*Pavelsky and Smith*, 2008]. The RMSE value also incorporates several other sources of error, including differences in discharge between the remotely sensed and in situ measurements and error in the in situ width measurements.

To avoid bias from outliers, we used the Theil-Sen median estimator [*Sen*, 1968] to derive a robust linear regression between NARWidth and in situ width measurements (Figure 2). Regression of in situ widths ≥ 100 m yields a slope that deviates by 3% from unity, but inclusion of all river width data (≥ 30 m) produces a slope that deviates by 16%. This deviation is expected because NARWidth is more likely to include overestimates of river width compared to underestimates where river width approaches the resolution of the Landsat imagery. For example, NARWidth never includes underestimates of 30 m wide rivers because they are narrower than one Landsat pixel, but it will include overestimates of these rivers. Goodness of fit ($r_s = 0.83$) was characterized using Spearman's nonparametric correlation coefficient [*Spearman*, 1904]. Overall, comparison with in situ measurements suggests that NARWidth provides, on average, an accurate representation of river widths at mean annual discharge to the extent that this is possible from Landsat imagery.

3.2. River Width Distributions

The NARWidth data set allows for the first analysis of the frequency distribution of river width measurements on a continental scale. The distribution of average river length binned by river width closely follows a power law of river width such that

$$\text{Length} = C \times \text{Width}^{-\alpha}, \tag{1}$$

where $C = 3.24 \times 10^{10}$ m$^{\alpha+1}$ and $\alpha = 2.18$ (Figure 3a). C and α were calculated using maximum likelihood estimation to avoid assumptions associated with regression analysis of binned data [*Clauset et al.*, 2009; *Gillespie*, 2014]. While other functions may also characterize the distribution of river widths, we use a power function because power laws are regularly used in hydraulic scaling and the curve closely fits the length of rivers from 100 to 2000 m wide ($r^2 > 0.996$, $p < 0.001$). Outside of this range, the function overestimates the length of rivers, particularly for the widest observed rivers where the distribution of river width appears to deviate from a power law spectrum. The upper tail, defined here as widths greater than 2000 m, is composed primarily of measurements from large, multichannel rivers. Sixty-three percent of rivers wider than 2000 m are from multichannel rivers compared to only 23% of rivers between 1000 and 2000 m wide. Geographically, multichannel rivers greater than 100 m wide make up 26.2% of all rivers north of 60°N while only composing 14.9% of rivers south of 60°N.

Although the river width distributions derived from the HYDRO1k DEM and NARWidth both closely fit power law functions, there are two key differences between them. First, the DEM-derived width distribution is
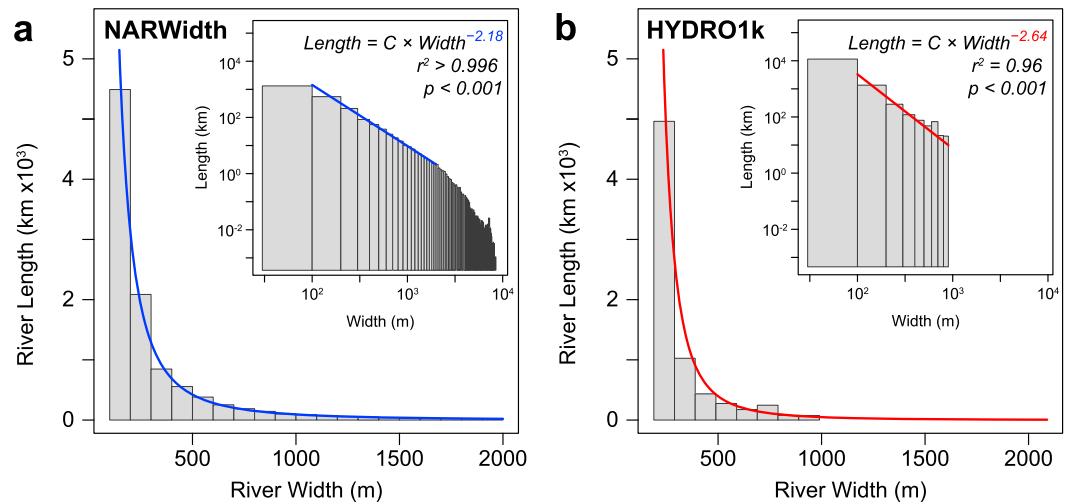
Figure 3. River width distributions from 100 to 2000 m. The insets show the full range of observed data in log space. Width distributions are described by a power function (equation (1)) with r^2 values estimated using a linear regression of log-binned data [*White et al.*, 2008]. (a) NARWidth-derived distribution, where $C = 3.24 \times 10^{10}\ m^{-1.18}$. (b) HYDRO1k DEM-derived distribution, where $C = 3.67 \times 10^{10}\ m^{-1.64}$.

characterized by a higher exponent ($\alpha = 2.64$ in equation (1)) than the NARWidth distribution ($\alpha = 2.18$), signifying that the DEM-derived data set contains a lower proportion of wide rivers (Figure 3b). Second, the DEM-derived data set does not include rivers wider than 894 m, resulting in a frequency distribution with a relatively truncated upper tail (Figure 3b inset).

3.3. Total Surface Area of North American Streams and Rivers

We used the distribution of total river surface area binned by width to estimate the overall surface area of all streams and rivers in North America (Figure 4). A power function closely describes the distribution of surface area of rivers 100 to 2000 m wide ($r^2 > 0.996$, $p < 0.001$) and is used to extrapolate surface area to rivers narrower than 100 m. The predictable surface area versus width relationship observed here is also likely to persist for these small streams, because Horton ratios relating stream order to stream width and total length apply down to first-order perennial streams [*Downing et al.*, 2012; *Morisawa*, 1962]. As surface area is the product of stream length and width, it should also scale as a power law down to first-order streams.

A considerable unknown is the appropriate lower width boundary of the surface area extrapolation. Studies that use DEMs to extract fluvial networks typically assume a critical threshold drainage area (or support area) ranging from 0.1 to 1 km^2, which correspond to river widths of ~0.8 m to 2 m [*Beighley and Gummadi*, 2011; *Butman and Raymond*, 2011]. Instead of a threshold in drainage area, we use a threshold in river width directly. The value of this lower width threshold substantially influences the surface area calculation because of the nonlinear relationship between river width and total channel length. The relationship between the lower width threshold (m) and the total surface area of North American rivers (km^2) is described by

$$\text{Total Surface Area} = 183{,}683 \times \text{Lower Width Threshold}^{-0.179} - 44{,}468. \tag{2}$$

This relationship only applies for lower width thresholds below 100 m, because above this width, equation (2) begins to deviate from the observed data. *Downing et al.* [2012] compiled a list of stream order versus mean width data from 46 perennial first-order stream segments worldwide and found that the median stream width is 1.6 ± 1.1 m (1σ confidence intervals). Using these widths as the lower width threshold in equation (2), the total surface area of permanently flowing North American rivers and streams is $1.24^{+0.39}_{-0.15} \times 10^5$ km^2 or $0.55^{+0.17}_{-0.07}$% of the terrestrial land surface. This surface area value is likely an underestimation of total river surface area because (1) it is based on the median first-order stream width rather than the average width at stream heads (streams as narrow as 0.18 m have been observed [*Zimmerman et al.*, 1967]) and (2) it excludes the surface area contribution of ephemeral streams, estimated to account for 2–3% of global river surface area [*Downing et al.*, 2012; *Raymond et al.*, 2013].

$$Area = 3.22 \times 10^4 \times Width^{-1.18}$$
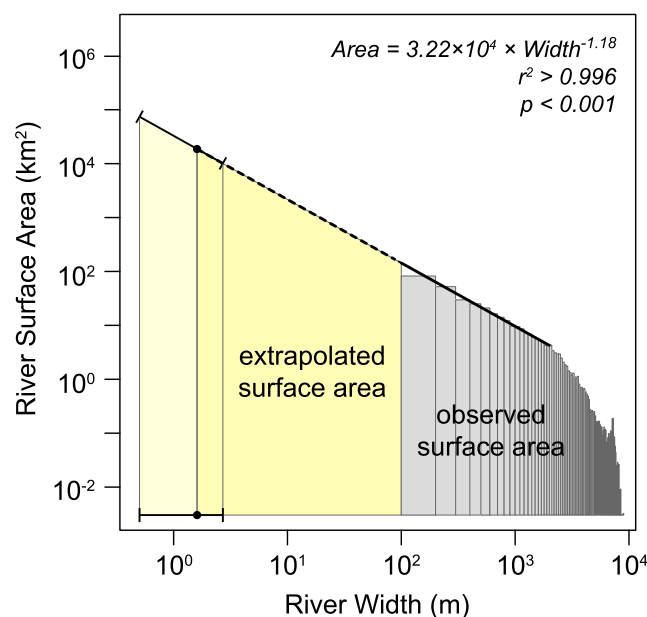$$r^2 > 0.996$$
$$p < 0.001$$

Figure 4. River surface area binned by river width. A power function was fit to data from widths 100 to 2000 m (solid line) and used to extrapolate total surface area of rivers less than 100 m wide (yellow polygon). The error bars denote the upper and lower width thresholds used in the surface area extrapolation (1.6 ± 1.1 m). The extrapolated surface area was then added to observed surface area (gray bars) to estimate the total river surface area of North America.

4. Discussion

4.1. Distribution of River Widths

Differences between NARWidth and the DEM-derived width data set likely arise from bias in measuring river width at gauge stations and oversimplifications involved in DHG scaling. The width-discharge relationship used to produce the DEM data set was developed using measurements largely collected at gauging stations [*Moody and Troutman*, 2002]. Stream gauges are typically located at stable, single-channel sites, often near bridges or other fixed structures, leading to a possible negative bias of measured river widths relative to the true width distribution [*Park*, 1977]. Because multichannel rivers tend to be wider and because their widths are more sensitive to changes in discharge than are single-channel rivers [*Smith et al.*, 1996], average river widths away from gauge stations may be underestimated if only widths at gauge stations are used. Given the nonlinear frequency distribution of river widths (equation (1) and Figure 3), this systematic underestimation of river width may result in an artificially high α value for the DEM-derived width distribution relative to the NARWidth distribution.

Additionally, DHG predicts that the maximum river width within a basin is located wherever discharge is greatest, usually at the basin outlet. Direct observations from Landsat imagery do not fully support this model. The widest width measurements in NARWidth are primarily from large, braided river systems flowing through floodplains (e.g., the Yukon and Mackenzie rivers (Figure 1)). These locations are examples of river form impacted by unusual physical conditions such as, in the case of braided rivers, abundant sediment supply [*Rosgen*, 1994]. Such physiographic conditions can result in substantial deviation from strict width-discharge relationships that are not captured by DHG. Thus, applying generic DHG scaling over large scales and differing river morphologies should be done with caution and, if possible, avoided.

4.2. River Surface Area Estimation

We estimated the total surface area of North American rivers by developing a relationship between river width and total surface area binned by width for rivers 100–2000 m wide, which we then use to extrapolate surface area for rivers narrower than 100 m (Figure 4). We based this extrapolation on classic Hortonian analysis which predicts that the distribution of river surface area will display statistical self-similarity at different spatial scales, indicating that similar processes act on river form over a wide range of channel sizes [*Rodríguez-Iturbe and Rinaldo*, 2001]. With decreasing basin size, however, hillslope and other local processes begin dominating, and the fractal relationships between total stream length and width must inevitably break down [*Benda et al.*, 2005]. We propose that the lower width threshold should be the geometric mean width at stream heads, but we are unaware of any robust quantitative information to constrain this value. Headwater stream networks are highly dynamic, largely dependent on changing hydrologic conditions [*Godsey and Kirchner*, 2014]. Further work is needed to quantify the distribution of river length, width, and discharge in headwater catchments to better constrain the frequency distributions of small streams that cannot be measured from remotely sensed data sets.

Previous estimates of river surface area across a large range of scales and physiographic conditions vary between 0.3% and 1.5% of watershed area, and our estimate of $0.55^{+0.17}_{-0.07}$% falls within this interval [*Davidson et al.*, 2010; *Downing et al.*, 2012; *Welcomme*, 1976]. In the contiguous United States, past estimates range from 0.52 to 0.56%, closely matching our estimate for the entire North American continent [*Butman and Raymond*, 2011; *Downing et al.*, 2012; *Leopold*, 1962]. Analyses of total global stream and river surface area estimate that rivers cover 0.30–0.56% of land surface [*Downing et al.*, 2012; *Raymond et al.*, 2013]. These studies rely on a relatively limited number of width measurements ($N < 1.0 \times 10^3$) to conduct stream order-scaling analysis. We avoid depending on potentially biased width-order analysis by building an extensive continental inventory of river width and length and analyzing the frequency distribution of surface area itself.

As part of a pioneering global carbon efflux study, *Raymond et al.* [2013] estimated that the total surface area of North American rivers is 0.46% of continental surface area. Raymond et al. estimated that on average, 14% of global surface area is frozen, and this fraction is removed from their analysis. They acknowledge that the impact of river ice on carbon efflux rates is poorly understood, and we do not attempt to account for the proportion of river surface area that is frozen. Noting this limitation of comparability between the surface area estimates, our likely conservative estimate of $0.55^{+0.17}_{-0.07}$%, which excludes streams narrower than 1.6 ± 1.1 m, is 20^{+38}_{-15}% larger than Raymond et al.'s value. Further, Raymond et al. extrapolated width-order relationships down to streams with a drainage area of ~0.1 km², amounting to a lower width threshold of less than 1 m [*Beighley and Gummadi*, 2011]. The discrepancy between river surface area estimates may arise from the DHG-based extrapolation methods employed by Raymond et al. Their evaluation relies on a global DHG formula that scales river width with regional discharge. Thus, many of the same problems in estimating river width discussed in section 4.1 may also apply to their estimate (e.g., underestimating the abundance of wide rivers). Our estimation of North American river surface area indicates that gaseous emissions from rivers should likely be revised upward compared to most recent estimates.

5. Summary and Conclusions

In this study we introduced the first fine-resolution, continental scale survey of river width. The NARWidth data set can be used for a wide variety of applications including hydrologic, hydrodynamic, biogeochemical, and landscape evolution modeling. The methods developed to produce NARWidth may also be applied to produce multitemporal width data sets that can be used to directly quantify absolute river discharge [*Gleason and Smith*, 2014]. This data set will have practical use for the Surface Water and Ocean Topography (SWOT) satellite mission, scheduled for launch in 2020, which will simultaneously measure variations in water surface elevation, width, and slope. NARWidth is the first installment of the Global River Width Data Set–Landsat, which will be the first fine-scale river width data set with fully global coverage.

Analysis of NARWidth indicates that the distribution of river width differs from that calculated by applying DHG scaling to DEM-derived basin areas. We find that the total surface area of North American rivers is $1.24^{+0.39}_{-0.15} \times 10^5$ km² or $0.55^{+0.17}_{-0.07}$% of total continental area, values 20^{+38}_{-15}% greater than the recent estimate by *Raymond et al.* [2013]. If underestimates from DHG-based surface area for North America also hold true for other continents, then global estimates of gaseous efflux from rivers to the atmosphere may also need to be revised upward. As width measurements for global rivers become available in the coming years, it will be possible to estimate global river surface area values using methods like the one presented here.

References

Allen, G. H., J. B. Barnes, T. M. Pavelsky, and E. Kirby (2013), Lithologic and tectonic controls on bedrock channel form at the northwest Himalayan front, *J. Geophys. Res. Earth Surf.*, *118*, 1806–1825, doi:10.1002/jgrf.20113.

Andreadis, K. M., G. J. P. Schumann, and T. M. Pavelsky (2013), A simple global river bankfull width and depth database, *Water Resour. Res.*, *49*, 7164–7168, doi:10.1002/wrcr.20440.

Bastviken, D., L. J. Tranvik, J. A. Downing, P. M. Crill, and A. Enrich-Prast (2011), Freshwater methane emissions offset the continental carbon sink, *Science*, *331*(6013), 50, doi:10.1126/science.1196808.

Beighley, R. E., and V. Gummadi (2011), Developing channel and floodplain dimensions with limited data: A case study in the Amazon Basin, *Earth Surf. Processes Landforms*, *36*(8), 1059–1071, doi:10.1002/esp.2132.

Benda, L., M. A. Hassan, M. Church, and C. L. May (2005), Geomorphology of steepland headwaters: The transition from hillslopes to channels, *J. Am. Water Resour. Assoc.*, *41*(4), 835–851, doi:10.1111/j.1752-1688.2005.tb03773.x.

Butman, D., and P. A. Raymond (2011), Significant efflux of carbon dioxide from streams and rivers in the United States, *Nat. Geosci.*, *4*(12), 839–842, doi:10.1038/ngeo1294.

Clauset, A., C. Shalizi, and M. Newman (2009), Power-law distributions in empirical data, *SIAM Rev.*, *51*(4), 661–703, doi:10.1137/070710111.

Davidson, E. A., R. O. Figueiredo, D. Markewitz, and A. K. Aufdenkampe (2010), Dissolved CO_2 in small catchment streams of eastern Amazonia: A minor pathway of terrestrial carbon loss, *J. Geophys. Res.*, 115, G04005, doi:10.1029/2009JG001202.

Downing, J. A., J. J. Cole, C. M. Duarte, J. J. Middelburg, J. M. Melack, Y. T. Prairie, P. Kortelainen, R. G. Striegl, W. H. McDowell, and L. J. Tranvik (2012), Global abundance and size distribution of streams and rivers, *Inland Waters*, 2(4), 229–236, doi:10.5268/IW-2.4.502.

Ferguson, R. I. (1986), Hydraulics and hydraulic geometry, *Prog. Phys. Geogr.*, 10(1), 1–31, doi:10.1177/030913338601000101.

Gillespie, C. S. (2014), Fitting heavy tailed distributions: The power law package, *R package version* 0.20.5, edited, Newcastle, U. K.

Gleason, C. J., and L. C. Smith (2014), Toward global mapping of river discharge using satellite images and at-many-stations hydraulic geometry, *Proc. Natl. Acad. Sci. U.S.A.*, doi:10.1073/pnas.1317606111.

Godsey, S. E., and J. W. Kirchner (2014), Dynamic, discontinuous stream networks: Hydrologically driven variations in active drainage density, flowing channels, and stream order, *Hydrol. Processes*, 28(23), 5791–5803, doi:10.1002/hyp.10310.

Gomez-Velez, J. D., and J. W. Harvey (2014), A hydrogeomorphic river network model predicts where and why hyporheic exchange is important in large basins, *Geophys. Res. Lett.*, 41, 6403–6412, doi:10.1002/2014gl061099.

GRDC (2011), *Long-Term Mean Monthly Discharges and Annual Characteristics of GRDC Station*, edited by G. R. D. Centre, Federal Institute of Hydrology (BfG), Koblenz, Germany.

Horton, R. E. (1945), Erosional development of streams and their drainage basins: Hydrophysical approach to quantitative morphology, *Geol. Soc. Am. Bull.*, 56(3), 275–370, doi:10.1130/0016-7606(1945)56[275:edosat]2.0.co;2.

Kiel, B. A., and M. B. Cardenas (2014), Lateral hyporheic exchange throughout the Mississippi River network, *Nat. Geosci.*, 7(6), 413–417, doi:10.1038/ngeo2157.

Kimbrough, R. A., R. R. Smith, G. P. Ruppert, and W. D. Wiggins (2003), Explanation of water-quality records, in *Water Data Report WA-03-1*, edited by USGS, p. 647, U.S. Geol. Surv., Vancouver, Wash.

Lague, D. (2014), The stream power river incision model: Evidence, theory, and beyond, *Earth Surf. Processes Landforms*, 39(1), 38–61, doi:10.1002/esp.3462.

Lehner, B., K. Verdin, and A. Jarvis (2008), New global hydrography derived from spaceborne elevation data, *Eos Trans. AGU*, 89(10), 93–94, doi:10.1029/2008eo100001.

Leopold, L. B. (1962), Rivers, *Am. Sci.*, 50(4), 511–537.

Leopold, L. B., and T. Maddock Jr. (1953), *The Hydraulic Geometry of Stream Channels and Physiographic Implications*, Rep., 252, 57 pp., U.S. Geol. Surv., Washington, D. C.

Li, J., and Y. Sheng (2012), An automated scheme for glacial lake dynamics mapping using Landsat imagery and digital elevation models: A case study in the Himalayas, *Int. J. Remote Sens.*, 33(16), 5194–5213, doi:10.1080/01431161.2012.657370.

Miller, Z. F., T. M. Pavelsky, and G. H. Allen (2014), Quantifying river form variations in the Mississippi Basin using remotely sensed imagery, *Hydrol. Earth Syst. Sci.*, 18(12), 4883–4895, doi:10.5194/hess-18-4883-2014.

Moody, J. A., and B. M. Troutman (2002), Characterization of the spatial variability of channel morphology, *Earth Surf. Processes Landforms*, 27(12), 1251–1266, doi:10.1002/esp.403.

Morisawa, M. E. (1962), Quantitative geomorphology of some watersheds in the Appalachian Plateau, *Geol. Soc. Am. Bull.*, 73(9), 1025–1046, doi:10.1130/0016-7606(1962)73[1025:qgoswi]2.0.co;2.

Neal, J., G. Schumann, and P. Bates (2012), A subgrid channel model for simulating river hydraulics and floodplain inundation over large and data sparse areas, *Water Resour. Res.*, 48, W11506, doi:10.1029/2012wr012514.

O'Loughlin, F., M. A. Trigg, G. J. P. Schumann, and P. D. Bates (2013), Hydraulic characterization of the middle reach of the Congo River, *Water Resour. Res.*, 49, 5059–5070, doi:10.1002/wrcr.20398.

Park, C. C. (1977), World-wide variations in hydraulic geometry exponents of stream channels: An analysis and some observations, *J. Hydrol.*, 33(1–2), 133–146, doi:10.1016/0022-1694(77)90103-2.

Pavelsky, T. M., and L. C. Smith (2008), RivWidth: A software tool for the calculation of river widths from remotely sensed imagery, *IEEE Geosci. Remote Sens. Lett.*, 5(1), 70–73, doi:10.1109/lgrs.2007.908305.

Pavelsky, T. M., G. H. Allen, and Z. F. Miller (2014a), Spatial patterns of river width in the Yukon River Basin, in *Remote Sensing of the Terrestrial Water Cycle*, pp. 131–141, John Wiley, Hoboken, N. J., doi:10.1002/9781118872086.ch8.

Pavelsky, T. M., M. T. Durand, K. M. Andreadis, R. E. Beighley, R. C. D. Paiva, G. H. Allen, and Z. F. Miller (2014b), Assessing the potential global extent of SWOT river discharge observations, *J. Hydrol.*, 519(Part B), 1516–1525, doi:10.1016/j.jhydrol.2014.08.044.

Raymond, P. A., et al. (2013), Global carbon dioxide emissions from inland waters, *Nature*, 503(7476), 355–359, doi:10.1038/nature12760.

Rodríguez-Iturbe, I., and A. Rinaldo (2001), *Fractal River Basins: Chance and Self-Organization*, Cambridge Univ. Press, Cambridge, U. K.

Rosgen, D. L. (1994), A classification of natural rivers, *Catena*, 22(3), 169–199, doi:10.1016/0341-8162(94)90001-9.

Sen, P. K. (1968), Estimates of the regression coefficient based on Kendall's tau, *J. Am. Stat. Assoc.*, 63(324), 1379–1389, doi:10.1080/01621459.1968.10480934.

Smith, L. C., B. L. Isacks, A. L. Bloom, and A. B. Murray (1996), Estimation of discharge from three braided rivers using synthetic aperture radar satellite imagery: Potential application to ungaged basins, *Water Resour. Res.*, 32(7), 2021–2034, doi:10.1029/96wr00752.

Spearman, C. (1904), The proof and measurement of association between two things, *Am. J. Psychol.*, 15(1), 72–101, doi:10.2307/1412159.

Strahler, A. N. (1957), Quantitative analysis of watershed geomorphology, *Eos Trans. AGU*, 38(6), 913–920, doi:10.1029/TR038i006p00913.

U.S. Geological Survey (2014), HYDRO1K documentation, edited by U.S. Geol. Surv.

Verdin, K. L., and J. P. Verdin (1999), A topological system for delineation and codification of the Earth's river basins, *J. Hydrol.*, 218(1–2), 1–12, doi:10.1016/S0022-1694(99)00011-6.

Wehrli, B. (2013), Biogeochemistry: Conduits of the carbon cycle, *Nature*, 503(7476), 346–347, doi:10.1038/503346a.

Welcomme, R. L. (1976), Some general and theoretical considerations on the fish yield of African rivers, *J. Fish Biol.*, 8(5), 351–364, doi:10.1111/j.1095-8649.1976.tb03964.x.

White, E. P., B. J. Enquist, and J. L. Green (2008), On estimating the exponent of power-law frequency distributions, *Ecology*, 89(4), 905–912, doi:10.1890/07-1288.1.

Wohl, E. (2004), Limits of downstream hydraulic geometry, *Geology*, 32(10), 897–900, doi:10.1130/g20738.1.

Xu, H. (2006), Modification of normalized difference water index (NDWI) to enhance open water features in remotely sensed imagery, *Int. J. Remote Sens.*, 27(14), 3025–3033, doi:10.1080/01431160600589179.

Yamazaki, D., F. O'Loughlin, M. A. Trigg, Z. F. Miller, T. M. Pavelsky, and P. D. Bates (2014), Development of the global width database for large rivers, *Water Resour. Res.*, 50, 3467–3480, doi:10.1002/2013wr014664.

Zimmerman, R. C., J. C. Goodlett, and G. H. Comer (1967), The influence of vegetation on channel form of small streams, in *Proceedings of the Symposium on River Morphology*, vol. 75, pp. 255–275, International Association of Scientific Hydrology, Wallinford, U. K.